

PAPER

[View Article Online](#)
[View Journal](#) | [View Issue](#)Cite this: *Dalton Trans.*, 2023, **52**, 3449Sohan Lal, ^a Richard J. Staples ^b and Jean'ne M. Shreeve ^{*,a}

Design and synthesis of phenylene-bridged isoxazole and tetrazole-1-ol based energetic materials of low sensitivity†

A variety of phenylene-bridged isoxazole and tetrazole-1-ol based green energetic materials was synthesized, for the first time, in good to excellent yields. The structures of the newly synthesized compounds were confirmed by spectroscopic techniques, elemental analysis, and single-crystal X-ray analysis. The value of the present work is that all newly synthesized compounds have good thermal stabilities ranging between 167–340 °C and acceptable densities between 1.51 g cm⁻³ to 1.82 g cm⁻³. Detailed computational insight into the energetic properties of the new compounds shows that they have good energetic properties (propulsive and ballistic) with excellent thermal and mechanical stabilities which makes them promising candidates for solid propulsion systems. Compounds **5**, **12** and **14** are the superior candidates as melt-castable energetic materials.

Received 18th January 2023,
Accepted 21st February 2023

DOI: 10.1039/d3dt00166k

rsc.li/dalton


Introduction

Energetic materials (EMs) attract extensive attention from the scientific community because of their wide range of applications as propellants, explosives, and pyrotechnics.^{1–4} In the last few decades many interesting, energetic materials have been designed and subsequently synthesized including octanitrocubane (ONC),⁵ 2,4,6,8,10,12-hexanitrohexaaza-isowurtzitane (CL-20),⁶ 4,10-dinitro-2,6,8,12-tetra-oxa-4,10-diazatetracyclo[5.5.0.0.5'.0.3.11]-dodecane (TEX),^{7a} formamidine nitroformate (FANF),^{7b} 1,3,5-trinitroperhydro-1,3,5-triazine (RDX),⁸ dihydroxylammonium-5,5'-bistetrazolyl-1,1'-diolate (TKX-50),⁹ and 1,3,5,7-tetranitro-1,3,5,7-tetrazocane (HMX).¹⁰ In addition to these well-known energetic compounds, a few aromatic energetic materials such as 2,4,6-trinitrobenzene-1,3,5-triamine (TATB),¹¹ 2,4,6-trinitrotoluene (TNT),¹¹ picric acid (PA),⁴ and 2,2',4,4',6,6'-hexanitrostilbene (HNS)¹² also attract the attention of materials chemists due to their high stability and good performance. In general, aromatic compounds with low oxygen balance, especially benzene-containing EMs are known to generate large amounts of soot during their combustion.¹³ However, this can be improved by introducing appropriate explosophoric groups (–NO₂, –ONO₂, –N₃ and –NHNO₂, etc.)

on the benzene core. Such EMs possess high positive enthalpies of formation and high density which are governed by their planar structures and high values of their packing coefficients. Some well-known aromatic energetic materials are given with their key performance properties in Fig. 1.

Excellent detonation properties of the bridged compounds make them ideal components for space and military applications.¹⁴ Some of these energetic materials with their key properties are shown in Fig. 2.^{9,15} However, the main concern associated with these compounds is their high sensitivity towards impact and friction, which restricts their real-life applications.

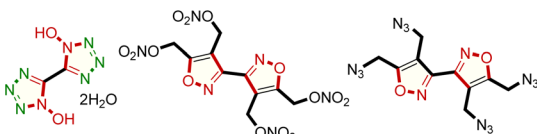
Melt-castable materials are a novel class of energetic materials, having melting temperatures in the range of 70–125 °C which are values significantly different from their decomposition temperatures. TNT- and dinitroanisole- (DNAN) based melt-castable eutectic formulations are well-known in the literature.¹⁶ However, environmental issues, low density



	TATB	TNT	HNS	DNAN
ρ (g/cm ³)	= 1.93	1.65	1.74	1.33
Dv (m/s)	= 8464	6824	7612	7020
IS (J)	= >50.0	>15.0	>5.0	>40
Mp (°C)	= 350	300	316	95

Fig. 1 Molecular structure and associated energetic properties of commonly used aromatic energetic materials.

^aDepartment of Chemistry, University of Idaho, Moscow, Idaho, 83844-2343, USA.E-mail: jshreeve@uidaho.edu; Fax: (+1) 208-885-5173^bDepartment of Chemistry, Michigan State University, East Lansing, Michigan 48824, USA† Electronic supplementary information (ESI) available. CCDC 2206847. For ESI and crystallographic data in CIF or other electronic format see DOI: <https://doi.org/10.1039/d3dt00166k>



	BTetz-ol	TNMBIO	TAMBIO
ρ (g/cm ³)	= 1.81	1.79	1.57
Dv (m/s)	= 8764	7847	7147
IS (J)	= >40	3.0	2.0
Mp/T _d	= 75/214	122/194	28/192

Fig. 2 Molecular structure and associated energetic properties of recently reported bistetrazole-1-ol and bis-isoxazole based energetic materials.^{9–15}

and poor explosive performance encourage an interest in the scientific community in designing and synthesizing new melt-castable energetic materials that address these concerns. Significant work has been carried out on the design, synthesis, and theoretical calculations of aromatic explosive/propellants. When designing a potential energetic material, performance as well as stability of the desired EM, is important.

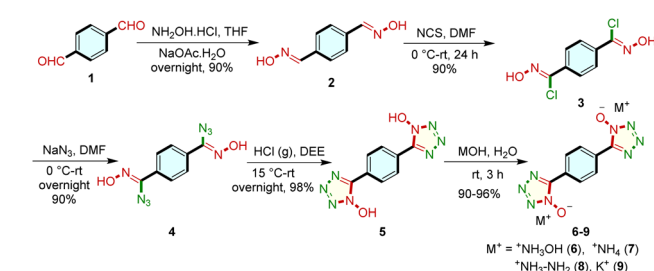
A benzene ring with appropriate explosophoric groups is a suitable basic skeleton to provide excellent density, high positive enthalpy of formation, good detonation performance and a π - π stacking interaction which leads to lower sensitivities compared to traditional energetic materials. Now the new compounds have been designed using a benzene ring as a basic skeleton, followed by introduction of azidomethyl ($-\text{CH}_2\text{N}_3$) and nitratomethyl ($-\text{CH}_2\text{ONO}_2$) groups to improve the nitrogen and oxygen content.

Results and discussion

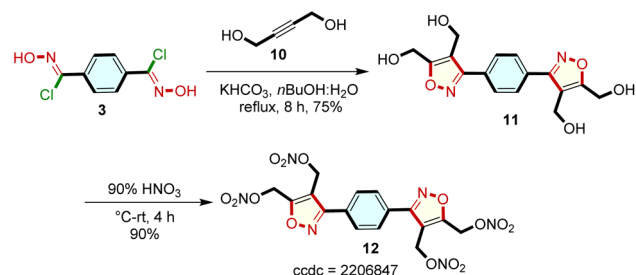
Synthesis

Terephthalaldehyde, **1**, is an excellent substrate for the syntheses of phenylene-bridged isoxazoles and tetrazole-*N*-oxide. Initially, chloro-oxime **3** was prepared *via* a literature procedure.¹⁷ Subsequently, it was converted into bis(azido-oxime) **4** by reacting with sodium azide in dimethylformamide (DMF) at ambient temperature. Then HCl(g) was added to the bis(azido-oxime) **4** which resulted in bis(tetrazole-1-ol) **5** in excellent yield. Further, to improve the energetic content, compound **5** was reacted with selected energetic bases such as hydroxylamine, ammonia, and hydrazine and for comparison with potassium hydroxide to form the potassium salt, **9** (Scheme 1).

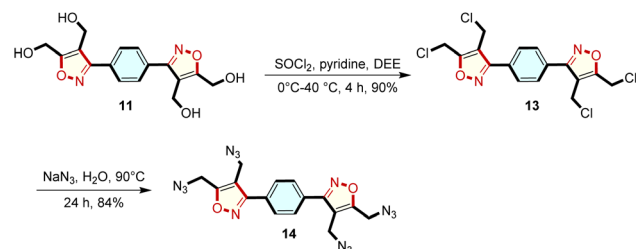
In another series, bis(chloro-oxime) **3** was treated with but-2-yne-1,4-diol **10** in the presence of potassium bicarbonate to give isoxazoles with tetramethyl alcohol **11** in excellent yields. Compound **11** was utilized as a key precursor for the synthesis of novel energetic compounds, namely 1,4-phenylenebis(isoxazole-3,4,5-triyl)-tetrakis(methylene)tetra-nitrate **12** (Scheme 2) and 1,4-bis(4,5-bis(azidomethyl)isoxazole-3-yl)-benzene **14** (Scheme 3). Compound **11** was nitrated with 90% HNO_3 at 0 °C to give compound **12** in excellent yield, 90% (Scheme 2).



Scheme 1 Synthesis of 5,5'-(1,4-phenylene) bis(1*H*-tetrazol-1-ol) (**5**) and its energetic salts (**6–9**).



Scheme 2 Synthesis of 1,4-bis(4,5-bis(nitratomethyl)isoxazol-3-yl)benzene (**12**).



Scheme 3 Synthesis of 1,4-bis(4,5-bis(azidomethyl)isoxazol-3-yl)benzene (**14**).

Compound **11** was treated with SOCl_2 in the presence of pyridine to form the corresponding tetrachloro derivative **13**, which was subsequently heated with sodium azide at 90 °C to give compound **14** in excellent yield, 84% (Scheme 3).

All the newly synthesized compounds have been fully characterized by ^1H , ^{13}C , and ^{15}N NMR, elemental analysis, and IR spectra. The structure of compound **12** was established by single crystal X-ray analysis (Fig. 3).

Crystal structure

Suitable single yellow plate-shaped crystals of compound **12** were obtained by slow evaporation of methanol.

Compound **12** (Fig. 3) crystallizes in the monoclinic space group $P21/c$ with a density of 1.697 g cm^{-3} at 100 K with a half molecule in the asymmetric unit, which is characterized by the sum formula – in other words Z is 2 and Z' is 0.5. Compound **12** was found to be packed in a planar structure and the distance between the two parallel layers is about 4.64 Å. The diagonal



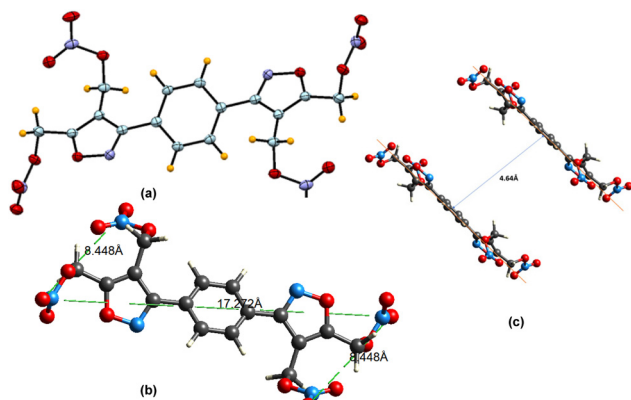


Fig. 3 Single crystal structure of compound **12** (CCDC = 2206847) (a) ORTEP diagram. (b) Diagonal length and width of the molecule. (c) Distance between two parallel layers.

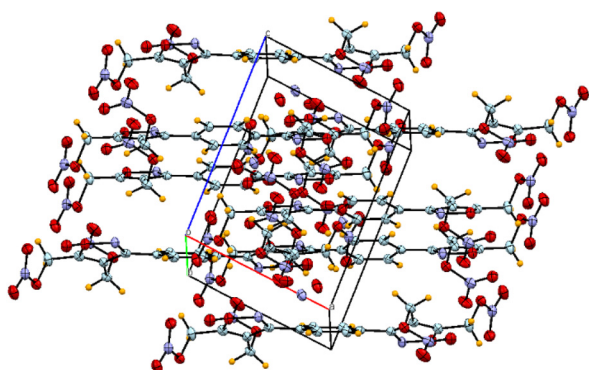


Fig. 4 Packing diagram of compound **12**.

length and width of the molecule were measured to be 17.27 Å and 8.44 Å, respectively. The packing diagram is shown in Fig. 4. The crystal data collection parameters and other useful crystallographic data are given in the ESI (Tables S4–S11†).

Computational methods

Ab initio-based computational insight into the title compounds was carried out at B3LYP/6-311++ G (d,p) (atomization method) and MP2/6-311++ G** (isodesmic method, at G2 level¹⁸) with the help of the Gaussian 03 suite of programs.¹⁹ The gas-phase enthalpies of formation ($\Delta H_f^\circ(\text{g})$) of the title compounds were calculated using their isodesmic equations. Then, their solid phase enthalpies of formation ($\Delta H_f^\circ(\text{s})$) were estimated from their gas phase enthalpy of formation ($\Delta H_f^\circ(\text{g})$) and enthalpy of sublimation (ΔH_{sub}) using Hess's law (eqn (1)).²⁰

$$\Delta H_f^\circ(\text{s}) = \Delta H_f^\circ(\text{g}) - \Delta H_{\text{sub}} \quad (1)$$

where $\Delta H_f^\circ(\text{s})$ is the solid-phase enthalpy of formation, $\Delta H_f^\circ(\text{g})$ is the gas phase enthalpy of formation and ΔH_{sub} is the enthalpy of sublimation.

The enthalpy of sublimation was estimated using Trouton's rule according to eqn (2).²¹

$$\Delta H_{\text{sub}} = 0.188 \times T / \text{kJ mol}^{-1} \text{ K}^{-1} \quad (2)$$

where, T , is either the melting point (mp) or the decomposition temperature (T_d), when no melting happens before decomposition.

For salts, the solid-state enthalpies of formation (ΔH_f°) were obtained using Born–Haber energy cycles.²² The experimental densities of the title compounds were determined at 25 °C using a gas pycnometer. Subsequently, using their solid phase enthalpies of formation ($\Delta H_f^\circ(\text{s})$) and experimental densities (Table 1), the related propulsive, ballistic and detonation performances were predicted using EXPLO5 V6.06 software.²³

The stabilities of the new compounds were estimated in terms of their electrostatic potentials (ESP), bond dissociation energies (BDEs) (eqn (3)), and energy difference between their HOMOs and LUMOs using B3LYP/6-311++ G (d,p) level of theory with Multiwfn and VMD softwares²⁴ and compared with the experimental stability (IS and FS) values.

$$\text{BDE} [\text{AB}] = E_0 [\text{A} \cdot] + E_0 [\text{B} \cdot] - E_0 [\text{AB}] \quad (3)$$

where, BDE [AB] is bond dissociation energy and $E_0 [\text{A} \cdot]$ and $E_0 [\text{B} \cdot]$ are the energies of individual homolytic part and $E_0 [\text{AB}]$ is the total energy of the individual molecule.

Densities of all newly synthesized compounds were determined with a gas pycnometer at 25 °C and found to be in the range of 1.51–1.82 g cm^{−3}. The potassium salt **9** has the highest density (1.82 g cm^{−3}) among salts **6**–**9**. It is notable that the relatively higher densities of neutral compounds **5**, **6**, **12** and **14** (1.63, 1.62, 1.63, and 1.60 g cm^{−3}, respectively), result from π – π stacking interactions and their planar structures. The existence of such extensive interactions among adjacent molecules which are confirmed based on the single crystal X-ray structures of compound **12**, resulted in their high densities, and are comparable to the well-known explosive TNT

Table 1 Comparison of physicochemical properties of **4**–**14** with RDX, TNT and HNS

Compd	Ω^{CO^a} (%)	N + O ^b [%]	ΔH_f^c [kJ mol ^{−1}]	ρ^d [g cm ^{−3}]	Mp/ T_d^e [°C]
4	−58.50	58.52	804.30	1.57	—/167
5	−58.50	58.52	775.02	1.63	99/209
6	−51.20	65.36	508.69	1.62	—/195
7	−68.50	61.40	381.76	1.58	—/251
8	−67.00	64.48	740.29	1.51	—/228
9	−39.70	44.69	−14.25	1.82	—/340
12	−122.10	60.12	−57.82	1.63	123/177
14	−74.00	52.75	1612.71	1.60	114/207
RDX ^f	0.0	81.06	70.3	1.80	—/204
TNT ^g	−24.70	60.76	−59.30	1.65	—/300
HNS ^h	−21.80	61.31	78.24	1.74	—/316

^a Oxygen balance based on CO. ^b Nitrogen and oxygen contents in percentage. ^c Calculated solid phase enthalpy of formation. ^d Measured densities, gas pycnometer at room temperature (25 °C). ^e Melting points and thermal decomposition temperature (onset) under nitrogen gas (DSC, 5 °C min^{−1}, see ESI†). ^f Ref. 10 and 25. ^g Ref. 11. ^h Ref. 12.



(1.65 g cm⁻³). Among the salts 6–9, compound 9 has a higher density than that of RDX ($\rho = 1.80$ g cm⁻³) as listed in Table 1.

All compounds are solid at room temperature and their decomposition temperatures are found between 167 °C to 340 °C (see ESI, Fig. S6, S13, S19, S26, S31, S38, S43, S49, S55 and S66†). All the title compounds 4–14 have high positive enthalpy of formation, except for compounds 9 and 12. The most positive enthalpy of formation obtained for the azido-methyl-isoxazole 14 (1612.71 kJ mol⁻¹) followed by the azido-oxime 4 (804.30 kJ mol⁻¹), are attributed to the azido groups in the molecules. The lowest ΔH_f° was obtained for the tetranitrate 12 (–57.82 kJ mol⁻¹).

Propulsive properties of the newly synthesized compounds

The suitability of the title compounds as solid propellants was evaluated by using EXPLO5 V6.06 software.²³ Their performances were evaluated with three different propellant formulations, viz., (i) monopropellants (neat); (ii) bi-propellants and composite propellants: propellant formulations with AP/HTPB; (iii) composite propellants: propellant formulations with GAP/DOA. As monopropellants, all the new compounds, except compounds 7 and 9, have considerably higher propulsive properties than that of TNT and lower than that of RDX.

A similar trend was also observed, when the performance of the new compounds (80%) was studied as composite-propellants with energetic binder GAP (17%) and plasticizer DOA (3%). With exception of the ammonium salt 7, and the potassium salt 9, all compounds show promising propulsion values ($I_{sp} = 218$ –224 s and $C^* = 1241$ –1272 m s⁻¹), which are better than those of TNT (~217 s and $C^* = 1235$ m s⁻¹), which suggest their potential use as solid composite propellants in the rocket industry (Table 2).

Additionally, two different composite propellant formulations with ammonium perchlorate (AP) and HTPB (i) 80% AP, 10% HTPB and 10% title compounds (ii) 80% AP and 20% new compounds, have been calculated and the results are listed in Table 2. The specific impulse (I_{sp}) of the title compounds were

comparable with that of TNT. However, when the title compounds were used as oxidizers instead of ammonium perchlorate (AP) in the propellant formulations (80% title compound: 20% HTPB), it was revealed that these compounds performed better than TNT but due to lack of oxygen content they had not performed as potential oxidizers (Table 2). Interestingly, in the other formulation with ethanol, the efficiency of ethanol as a fuel can be significantly improved by adding the new compounds (20%) as fuel supplements. The specific impulse (I_{sp}) and vacuum specific impulse ($I_{sp,vac}$) of the fuel blends were improved by 10–29 s and 13–33 s, respectively as given in Table 2.

The suitability of newly synthesized energetic materials as explosives was evaluated using their calculated ΔH_f° and measured room temperature densities with EXPLO5 V6.06 software (Table 3).

The highest detonation performance values were observed for compound 6 (DP = 19.98 GPa and $D_v = 7491$ m s⁻¹) and compound 12 (DP = 18.98 GPa and $D_v = 6865$ m s⁻¹) and are superior to that of TNT. Since all the compounds possess lower detonation performances than RDX, they can be considered safe to use as solid propellants (Table 3).

Table 3 Comparison of the sensitives and detonation properties of 4–14 with TNT, FANF and RDX

Compd	DP ^a [GPa]	Dv ^b [m s ⁻¹]	Q ^c [kJ kg ⁻¹]	IS ^d [J]	FS ^e [N]
4	17.86	6693.04	4404.38	≥10	≥240
5	17.16	6885.27	4314.17	≥40	≥360
6	19.98	7491.57	4228.68	≥40	≥360
7	16.86	7105.19	2913.26	≥40	≥360
8	18.35	7371.84	3875.11	≥40	≥360
9	11.49	5596.02	1822.33	≥40	≥360
12	18.98	6865.72	4689.51	≥15	≥360
14	17.11	6621.19	4149.31	≥15	≥360
TNT ^f	18.56	6839.96	4395.70	≥15	≥353
RDX ^f	34.00	8867.06	5728.99	≥7.5	≥120
FANF ^g	34.13	8811.00	—	≥100	≥360

^a Calculated detonation pressure. ^b Calculated detonation velocity. ^c Heat of detonation. ^d Measured impact sensitivity (IS). ^e Measured friction sensitivity (FS). ^f Ref. 10. ^g Ref. 7b.

Table 2 Propulsive properties of compound 4–14 in comparison with TNT and RDX

#	$I_{sp,vac}$ ^a [s]	$\rho I_{sp,vac}$ ^b [g cm ⁻³ s]	C^* ^c [m s ⁻¹]	$I_{sp,vac}$ ^d [s]	$\rho I_{sp,vac}$ ^e [g cm ⁻³ s]	C^* ^f [m s ⁻¹]	$I_{sp,vac}$ ^g [s]	$\rho I_{sp,vac}$ ^h [g cm ⁻³ s]	$I_{sp,vac}$ ⁱ [s]	$\rho I_{sp,vac}$ ^j [g cm ⁻³ s]	I_{sp} ^k [s]	$I_{sp,vac}$ ^l [s]
4	232.35	364.79	1310	224.66	333.60	1272	267.04	457.09	206.52	282.21	146.51	159.35
5	229.33	373.82	1294	222.31	339.56	1258	266.74	458.42	204.24	286.44	145.84	158.58
6	229.15	371.22	1308	222.88	338.87	1264	267.58	459.58	206.80	288.82	146.80	159.49
7	198.29	313.30	1109	198.67	296.42	1109	263.32	451.04	183.04	251.24	138.49	150.03
8	225.37	340.31	1276	220.04	317.19	1241	266.23	453.73	204.24	271.58	144.96	157.32
9	142.88	260.04	760	160.25	265.54	853	260.72	453.06	138.22	208.86	130.96	142.05
12	230.59	375.86	1337	223.31	341.09	1277	269.11	462.49	206.50	289.61	149.17	162.45
14	223.20	357.13	1245	218.05	328.43	1224	265.28	455.01	200.27	277.30	144.70	157.32
TNT	222.56	368.12	1284	217.07	335.20	1235	268.36	461.90	200.55	284.10	147.37	160.38
RDX	286.98	516.56	1651	259.81	427.08	1528	273.76	475.06	234.12	351.19	155.44	169.27

^a $I_{sp,vac}$ = vacuum specific impulse at 100% compound (neat). ^b $\rho I_{sp,vac}$ = density vacuum specific impulse at 100% compound (neat). ^c Characteristic velocity at 100% compound (neat). ^d $I_{sp,vac}$ = vacuum specific impulse at compound (80%), 17% (GAP) and DOA (3%). ^e $\rho I_{sp,vac}$ = density vacuum specific impulse at compound (80%), 17% (GAP) and DOA (3%). ^f Characteristic velocity at compound (80%), 17% (GAP) and DOA (3%). ^g $I_{sp,vac}$ = vacuum specific impulse at 80% AP, 10% binder (HTPB) and 10% compound. ^h $\rho I_{sp,vac}$ = density vacuum specific impulse at 80% AP, 10% binder (HTPB) and 10% compound. ⁱ $I_{sp,vac}$ = vacuum specific impulse at 80% compound and 20% HTPB. ^j $\rho I_{sp,vac}$ = density vacuum specific impulse at 80% compound and 20% HTPB. ^k I_{sp} = specific impulse at compound (20%), and ethanol (80%). ^l $I_{sp,vac}$ = vacuum specific impulse at compound (20%), and ethanol (80%), for 100% ethanol $I_{sp} = 120.09$ s and $I_{sp,vac} = 129.46$ s.



The new compounds as solid propellants were further ensured to be suitable by measuring their impact sensitivity (IS) and friction sensitivity (FS) with the help of a BAM Fallhammer apparatus and a BAM friction tester,²⁶ respectively. All the new compounds except for **4**, **12**, and **14** have sensitivities in the range of insensitive energetic materials. However, compounds **4** (IS = 10J, FS = 240N), **12** (IS = 15J, FS = 360N) and **14** (IS = 15J, FS = 360N) can be considered to be more sensitive energetic materials. The new compounds were dissolved in water and held at room temperature for two days. No decomposition was observed.

Furthermore, to understand the structure properties and intermolecular interactions in the crystal packing of compound **12**, its Hirshfeld surfaces and two-dimensional fingerprints were calculated by using CrystalExplorer 21.5.²⁷ Red and blue dots on the Hirshfeld surfaces demonstrate the high and low close interactions within the crystal (Fig. 5). The O...H (50%) and N...H (4%) interactions provide the extra stability to the molecules whereas O...N (5%), O...C (5%) and N...N (3%) are indications of good π - π stacking interactions in the molecules. Similarly, O...O (19%) arising from the oxygen atoms of nitrate ($-\text{ONO}_2$) groups are contributing to the high density and higher sensitivity of the molecules.

The O...H, N...H, O...N and O...C interactions are dominating over O...O interactions which suggests that compound **12** is a well stabilized compound. The kinetic stabilities of the newly synthesized compounds were predicted with the help of electrostatic potential (ESP) measurements as shown in Fig. 6. The global ESP maxima and minima are shown in small gold spheres and small blue spheres, respectively.

The high stability of compounds **12** and **14** is strongly supported by hydrogen bonds, van der Waals interactions and steric effects as shown in Fig. 7.

Compounds **4** and **5** have slightly higher ESP maxima (+53.55 and +68.57 kcal mol⁻¹, respectively) and compounds **5**, **12** and **14** have significantly lower global ESP minima (-37.52, -23.09, -30.46 kcal mol⁻¹, respectively) compared to RDX (+50.01 and -20.81 kcal mol⁻¹) and TNT (+38.66 and -22.39 kcal mol⁻¹), suggesting that the stability order of the

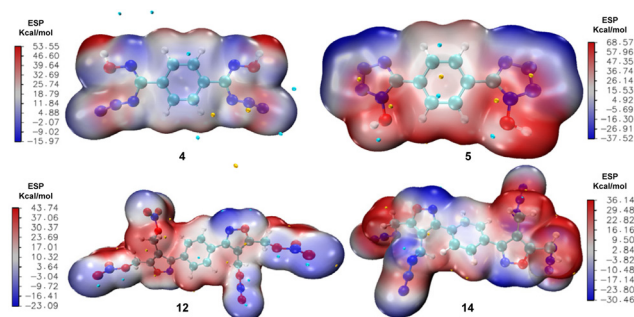


Fig. 6 Electrostatic potential (ESP) maps with the representation of surface maxima (small gold spheres) and minima (small blue spheres).

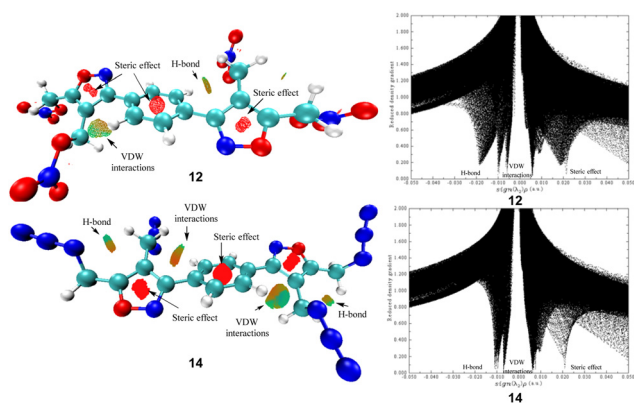


Fig. 7 Non-covalent interaction (NCI): reduced density gradient (RDG) and scatter diagram of compounds **12** and **14**.

selected compounds is $5 > \text{TNT} > 14 > \text{RDX} > 12 > 4$. The product of σ_{tot}^2 and balance of charges (ν) suggest that the stability of compounds **4** and **12** would be lower than that of RDX and TNT and that compound **5** will be most stable compound.

Similar trends also are found in their bond dissociation energies and the energy difference between their HOMO and LUMO orbitals as listed in Table 4.

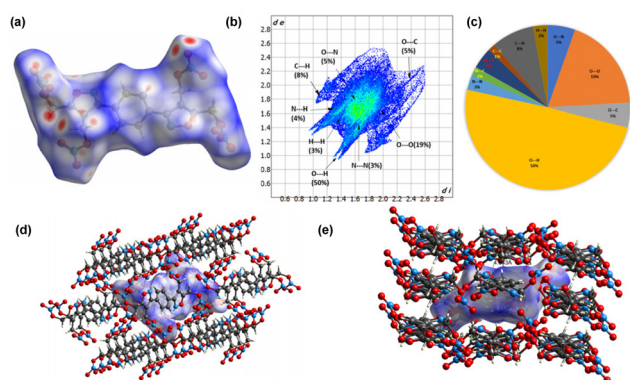


Fig. 5 (a) Hirshfeld surface graph. (b) 2D fingerprint plots in crystal stacking (c) individual atomic contacts percentage in the bar graphs and (d and e) the closest atoms in compound **12**.

Table 4 Comparison of ratio of positive and negative ESPs and the surface area of ESPs of compounds, σ_{tot}^2 , HOMO–LUMO energy gaps and BDE values

#	SA _{tot} ^a Å ²	Ratio ^b (%)	Ratio ^c (%)	σ_{tot}^2 ^d (kcal mol ⁻¹) ²	BDE ^e (kJ mol ⁻¹)	Ω ^f (eV)
4	263.46	42.63	57.37	13.58	23.58	4.186
5	248.04	65.31	34.69	61.63	510.37	4.679
12	480.30	59.58	40.42	20.11	126.03	4.818
14	448.86	57.15	42.85	28.92	231.51	5.115
RDX	209.49	55.74	44.26	27.29	130.85	5.993
TNT	221.89	57.88	42.12	22.48	238.45	4.926

^a SA_{tot} = total surface area. ^b Ratio of positive ESPs. ^c Ratio of negative ESPs. ^d Product of total variance and balance of charges. ^e Bond dissociation energies of trigger bond. ^f Energies difference between HOMO and LUMO orbitals.



Conclusions

Phenylene-bridged isoxazole and tetrazole-1-ol-based green energetic materials were obtained for the first time from readily available terephthalaldehyde in three to five steps in good to excellent yields. The structures of the newly synthesized compounds were established by ^1H , ^{13}C and ^{15}N NMR and IR spectra and elemental analysis. Additionally, the X-ray diffraction structure analysis of compound **12** further confirmed its synthesis. Differential scanning calorimetry and thermogravimetric analysis measurements suggest that all the new compounds are thermally and hydrolytically stable and possess good impact and friction sensitivities. They show excellent propulsive and detonation performance. Most of the new compounds are suitable candidates as solid rocket monopropellants and composite propellants for space-related applications. Compounds **6** (DP = 19.98 GPa, Dv = 7492 m s $^{-1}$) and **12** (DP = 18.98 GPa, Dv = 6866 m s $^{-1}$) were found to be the best candidates in this series. Compounds **5**, **12**, and **14** are the best choices as melt-castable energetic materials.

Experimental section

General methods

All reagents and solvents were used as received unless otherwise specified (AKSci, Sigma-Aldrich, Acros Organics, VWR). The FT-IR spectra were recorded with KBr plates on a Thermo Nicolet AVATAR 370 spectrometer. Densities were measured at 25 °C with a Micromeritics Accupyc II 1340 gas pycnometer. The melting and decomposition (onset) temperatures were obtained on a differential scanning calorimeter (TA Instruments Company, Model: Q2000) and thermogravimetric analysis (TGA, TA Instruments Company, Model: Q50). The samples were heated from 35 °C to 400 °C at the heating rate of 5 °C min $^{-1}$. ^1H and ^{13}C NMR spectra were recorded on a 300 MHz (Bruker AVANCE 300) nuclear magnetic resonance spectrometer operating at 300.13 and 75.48 MHz, respectively by using DMSO- d_6 as the solvent and locking solvent. The ^{15}N NMR spectra were recorded on a 500 MHz (Bruker AVANCE 500) nuclear magnetic resonance spectrometer operating at 50.70 MHz. The chemical shifts are given relative to tetramethylsilane (^1H , ^{13}C) and nitromethane (^{15}N) as external standards. Elemental analyses (C, H, N) were performed on a Vario Micro cube Elemental Analyser. The friction sensitivities (FS) and impact sensitivities (IS) were measured with a standard BAM friction tester and BAM drop hammer.

The crystals of compound **12** were mounted on a nylon loop with Paratone oil on a XtaLAB Synergy, Dualflex, HyPix diffractometer at 100 K. The structures were solved with the ShelXT²⁸ solution program using dual methods and by using Olex2.²⁹ The model was refined with ShelXL29 using full matrix least squares minimization on F^2 .

Caution! The new compounds are potentially high-energy materials and could detonate unpredictably under certain conditions. Therefore, it is strongly recommended that during the

experiments and their studies proper protective measures, such as Kevlar gloves, face shields, ear protection, and eye protection, should be taken at all times. Only small-scale reactions should be undertaken.

Synthesis of terephthalaldehyde dioxime (2).¹⁷ A suspension of compound **1** (6.70 g, 50.0 mmol, 1.0 equiv.) in tetrahydrofuran (50 mL) was cooled to 0 °C. To this cooled solution, hydroxylamine hydrochloride (7.700 g, 110.0 mmol, 2.2 equiv.) and sodium acetate (14.96 g, 110 mmol, 2.2 equiv.) were added slowly at 0 °C. The reaction mixture was allowed to warm gradually to room temperature and stirred overnight. After completion of the reaction, the tetrahydrofuran was evaporated and the resulting mixture was diluted with water (100 mL) and filtered to obtain dioxime **2**, which was further purified by recrystallization with ethanol. Pale yellow solid. 7.38 g, 90%, DSC (5 °C min $^{-1}$): 213 °C. IR (KBr, cm $^{-1}$) 3168 (s), 2987 (s), 2899 (s), 2763 (s), 1682 (m), 1624 (m), 1518 (m), 1456 (m), 1406 (w), 1323 (s), 1295 (s), 1213 (m), 980 (s), 858 (s), 821 (m), 531 (m). ^1H NMR (DMSO- d_6 , 300 MHz) δ 7.60 (s, 4H), 8.14 (s, 2H), 11.32 (s, 2H). ^{13}C NMR (DMSO- d_6 , 75.48 MHz) δ 126.8, 133.9, 147.9. Elemental analysis calcd (%) for C₈H₈N₂O₂ (164.16): C 58.53, H 4.91, N 17.06. Found: C 58.53, H 4.97, N 16.69.

Synthesis of *N*'1,*N*'4-dihydroxyterephthalimidoyl dichloride (3).¹⁷ A suspension of compound **2** (6.560 g, 40.0 mmol, 1.0 equiv.) in DMF (50 mL) cooled to 0 °C. *N*-Chlorosuccinimide (11.750 g, 88.0 mmol, 2.2 equiv.) was added portion-wise at 0 °C. The resulting reaction mixture was allowed to warm gradually to room temperature and stirred for 24 h. After completion of the reaction, ice-cold water was added to the reaction mixture to obtain a white precipitate immediately. This was filtered giving chloro-dioxime **3**, which was further purified by recrystallization from ethanol. White solid. 8.40 g, 90%, DSC (5 °C min $^{-1}$): 198 °C. IR (KBr, cm $^{-1}$) 3281 (s), 3144 (s), 3018 (s), 2898 (s), 1686 (m), 1648 (s), 1507 (m), 1434 (m), 1435 (m), 1401 (m), 1383 (m), 1250 (m), 1194 (w), 1107 (w), 1008 (s), 933 (s), 836 (s), 666 (w). ^1H NMR (DMSO- d_6 , 300 MHz) δ 7.67 (br s, 4H), 12.36 (s, 2H). ^{13}C NMR (DMSO- d_6 , 75.48 MHz) δ 126.9, 134.1, 134.9. Elemental analysis calcd (%) for C₈H₆Cl₂N₂O₂ (233.05): C 41.23, H 2.60, N 12.02. Found: C 42.25, H 2.91, N 12.35.

Synthesis of *N*'1,*N*'4-dihydroxyterephthalimidoyl diazide (4). Compound **3** (2.33 g, 10.0 mmol, 1.0 equiv.) was added to DMF (50 mL) followed by sodium azide (2.60 g, 40.0 mmol, 4.0 equiv.) added portion-wise to this mixture. The resulting mixture was allowed to warm gradually to room temperature and stirred overnight. After completion of the reaction, ice-cold water was added to give a white precipitate, which was removed by filtration to give azido-dioxime **4**, which was further purified by recrystallization from ethanol. White solid. 2.21 g, 90%, DSC (5 °C min $^{-1}$): 167 °C. IR (KBr, cm $^{-1}$) 3165 (s), 2198 (m), 2135 (s), 2085 (m), 1604 (m), 1412 (w), 1386 (w), 1323 (s), 1039 (m), 967 (s), 862 (m), 614 (w). ^1H NMR (DMSO- d_6 , 300 MHz) δ 7.69 (s, 4H), 11.89 (s, 2H). ^{13}C NMR (DMSO- d_6 , 75.58 MHz) δ 125.7, 132.0, 141.0. Elemental analysis calcd (%) for C₈H₆N₈O₂ (246.19): C 39.03, H 2.46, N 45.52. Found: C 39.07, H 2.76, N 45.34.



Synthesis of 5,5'-(1,4-phenylene)bis(1H-tetrazol-1-ol) (5). A suspension of compound 4 (2.460 g, 10.0 mmol, 1.0 equiv.) in diethyl ether (150 mL) was cooled to 0 °C. HCl(g) was bubbled through the suspension while the temperature was maintained below 15 °C, until the ether solution was saturated. Then it was maintained at room temperature overnight. After completion of the reaction, diethyl ether was evaporated and a white precipitate was formed, and separated by filtration. The solid was washed with acetonitrile and dried under air to give compound 5 as a dihydrate. White solid. 2.76 g, 98%, DSC (5 °C min⁻¹): 98 °C (mp), 208 °C (dec.). IR (KBr, cm⁻¹) 3295 (br s), 1906 (s), 1469 (s), 1384 (s), 1290 (s), 1258 (s), 1129 (s), 1010 (m), 842 (m), 735 (m), 687 (m), 623 (m), 563 (w). ¹H NMR (DMSO-d₆, 300 MHz) δ 8.34 (s, 4H). ¹³C NMR (DMSO-d₆, 75.48 MHz) δ 125.3, 128.3, 145.2. ¹⁵N NMR (50.70 MHz, DMSO-d₆): δ -3.1, -16.6, -55.2. Elemental analysis calcd (%) for C₈H₁₀N₈O₄ (282.22): C 34.29, H 2.88, N 39.99. Found: C 34.29, H 3.01, N 39.12.

General procedure for the synthesis of energetic salts (6–9). Compound 5 (846 mg, 3.0 mmol, 1.0 equiv.) was suspended in water (10 mL) and 50% hydroxylamine (792 mg, 12.0 mmol, 4.0 equiv.), ammonia (37% solution 10 mL, excess), or 98% hydrazine monohydrate (613 mg, 12.0 mmol, 4.0 equiv.) or potassium hydroxide (353 mg, 6.3 mmol, 2.1 equiv.) was added. The mixture was stirred at room temperature for 3 h, and the water was evaporated. The remaining solid was dissolved in acetonitrile and stirred at room temperature for 10–15 min. The precipitate was formed and collected by filtration to form white crystals of compound 6–8 and red brown crystals of compound 9.

Dihydroxylammonium-5,5'-(1,4-phenylene)bis(1H-tetrazol-1-olate) (6). White solid. 900 mg, 96%, DSC (5 °C min⁻¹): 195 °C (dec.). IR (KBr, cm⁻¹) 3415 (s), 3183 (s), 2995 (s), 2917 (s), 2708 (s), 1622 (m), 1524 (m), 1460 (s), 1384 (m), 1359 (m), 1280 (m), 1203 (s), 1130 (s), 1005 (m), 853 (m), 753 (w), 730 (w). ¹H NMR (DMSO-d₆, 300 MHz) δ 8.45 (s, 4H), 9.33 (br s, 4H). ¹³C NMR (DMSO-d₆, 75.48 MHz) δ 125.8, 126.3, 141.2. ¹⁵N NMR (50.70 MHz, DMSO-d₆): δ -12.6, -15.5, -59.4, -89.9, -297.4. Elemental analysis calcd (%) for C₈H₁₂N₁₀O₄ (312.25): C 30.77, H 3.87, N 44.86. Found: C 31.67, H 3.83, N 44.54.

Diammonium-5,5'-(1,4-phenylene)bis(1H-tetrazol-1-olate) (7). White solid. 755 mg, 90%, DSC (5 °C min⁻¹): 251 °C (dec.). IR (KBr, cm⁻¹) 3420 (s), 3139 (s), 3044 (s), 1705 (m), 1679 (m), 1614 (m), 1451 (s), 1398 (s), 1358 (s), 1295 (w), 1237 (s), 1118 (w), 1002 (w), 860 (w), 753 (w), 727 (w). ¹H NMR (DMSO-d₆, 300 MHz) δ 7.76 (br s, 8H), 8.44 (s, 4H). ¹³C NMR (DMSO-d₆, 75.48 MHz) δ 125.5, 126.4, 141.0. Elemental analysis calcd (%) for C₈H₁₂N₁₀O₂·2H₂O (316.28): C 30.38, H 5.10, N 44.29. Found: C 30.95, H 4.76, 43.68.

Dihydrazinium-5,5'-(1,4-phenylene)bis(1H-tetrazol-1-olate) (8). White solid. 875 mg, 94%, DSC (5 °C min⁻¹): 195 °C (dec.). IR (KBr, cm⁻¹) 3247 (s), 3174 (s), 2885 (s), 2743 (s), 2641 (s), 1631 (s), 1530 (s), 1454 (s), 1381 (s), 1355 (s), 1296 (s), 1261 (m), 1240 (s), 1147 (s), 1112 (s), 1003 (m), 969 (s), 848 (m), 752 (w), 725 (w), 525 (w), 467 (w). ¹H NMR (DMSO-d₆, 300 MHz) δ 6.00 (br s, 10H), 8.50 (s, 4H). ¹³C NMR (DMSO-d₆, 75.48 MHz) δ

125.5, 126.6, 140.6. ¹⁵N NMR (50.70 MHz, DMSO-d₆): δ -14.9, -15.5, -60.4, -84.6, -108.3, 331.1. Elemental analysis calcd (%) for C₈H₁₄N₁₂O_{2.4}H₂O (382.34): C 25.13, H 5.80, N 43.96. Found: C 25.15, H 5.48, N 43.24.

Dipotassium-5,5'-(1,4-phenylene)bis(1H-tetrazol-1-olate) (9). White solid. 990 mg, 92%, DSC (5 °C min⁻¹): 340 °C (dec.). IR (KBr, cm⁻¹) 3493 (s), 3418 (s), 3097 (w), 1557 (s), 1453 (s), 1385 (s), 1361 (s), 1300 (m), 1252 (m), 1226 (s), 1104 (s), 990 (m), 847 (m), 755 (m), 728 (m), 532 (m), 465 (m). ¹H NMR (DMSO-d₆, 300 MHz) δ 8.49 (s, 4H). ¹³C NMR (DMSO-d₆, 75.48 MHz) δ 124.8, 126.7, 140.0. Elemental analysis calcd (%) for C₈H₄K₂N₈O₂ (322.37): C 29.81, H 1.25, N 34.76. Found: C 29.07, H 1.29, N 42.34.

Synthesis of (1,4-phenylenebis(isoxazole-3,4,5-triyl))tetra-methanol (11). A mixture of compound 3 (2.33 g, 10.0 mmol, 1.0 equiv.), but-2-yn-1,4-diol (3.44 g, 40.0 mmol, 4.0 equiv.) and potassium bicarbonate (3.0 g, 30.0 mmol, 3.0 equiv.) in *n*-butanol (100 mL) was refluxed for 8 h. After completion of the reaction, the mixture was cooled and the solvent was removed under air and ice-cold water was added. A brown precipitate was removed by filtration and washed with cold water. The crude residue was purified by recrystallization with ethanol to give pure tetra-ol 11. White solid. 2.50 g, 75%, DSC (5 °C min⁻¹): 216 °C. IR (KBr, cm⁻¹) 3306 (br s), 2939 (s), 2869 (s), 1623 (s), 1429 (s), 1362 (s), 1320 (m), 1287 (s), 1188 (s), 1120 (w), 1040 (s), 1001 (s), 924 (s), 856 (m), 771 (s), 677 (m), 635 (w). ¹H NMR (DMSO-d₆, 300 MHz) δ 4.50 (s, 4H), 4.68 (s, 4H), 5.34 (br s, 2H), 5.59 (br s, 2H), 8.02 (s, 4H). ¹³C NMR (DMSO-d₆, 75.48 MHz) δ 51.4, 53.3, 114.6, 128.6, 130.3, 161.4, 170.3. Elemental analysis calcd (%) for C₁₆H₁₆N₂O₆ (332.31): C 57.83, H 4.85, N 8.43. Found: C 57.91, H 5.12, N 7.55.

Synthesis of (1,4-phenylenebis(isoxazole-3,4,5-triyl))-tetra-kis-(methylene)-tetranitrate (12). Compound 11 (996 mg, 3.0 mmol, 1.0 equiv.) was added slowly to 90% HNO₃ (6.0 mL) at 0 °C. The resulting reaction mixture was stirred for 4 h at the same temperature. After completion of the reaction (monitored by TLC), the reaction mixture was poured into ice-cold water and stirred for 15 min, filtered and dried *in vacuo* to give compound 12 which was purified by recrystallization with methanol. Yellow solid. 1.38 g, 90%, DSC (5 °C min⁻¹): 123 °C (mp), 177 °C (dec.). IR (KBr, cm⁻¹) 2910 (m), 1637 (s), 1463 (m), 1433 (s), 1366 (s), 1276 (s), 999 (m), 967 (s), 948 (s), 914 (s), 858 (s), 798 (s), 751 (s), 733 (w), 668 (m), 547 (w). ¹H NMR (DMSO-d₆, 300 MHz) δ 5.75 (s, 4H), 6.02 (s, 4H), 7.93 (m, 4H). ¹³C NMR (DMSO-d₆, 75.48 MHz) δ 63.3, 63.4, 110.4, 128.9, 129.2, 161.7, 165.4. ¹⁵N NMR (50.70 MHz, DMSO-d₆): δ -3.6, -43.2, -45.0. ¹⁴N NMR (36.14 MHz, DMSO-d₆): δ -44.1. Elemental analysis calcd (%) for C₁₆H₁₂N₆O₁₄ (512.30): C 37.51, H 2.36, N 16.40. Found: C 37.85, H 2.69, N 15.85.

Synthesis of 1,4-bis(4,5-bis(chloromethyl)isoxazol-3-yl)-benzene (13). A solution of compound 11 (996 mg, 3.0 mmol) in diethyl ether (20 mL) was added slowly to a mixture of SOCl₂ (1.785 g, 1.0 mL, 15.0 mmol, 5.0 equiv.) and pyridine (1.185 g, 1.2 mL, 15.0 mmol, 5.0 equiv.) at 0 °C. The mixture was heated at 40 °C for 4 h. Then it was allowed to cool gradually to room temperature. The excess SOCl₂ and pyridine was



removed under vacuum to leave a crude brown product **13** which was further purified by washing with water followed by trituration with hexane and diethyl ether. Brown solid. 1.10 g, 90%, DSC (5 °C min⁻¹): 160 °C. IR (KBr, cm⁻¹) 3017 (m), 2969 (m), 1706 (m), 1628 (s), 1537 (m), 1487 (m), 1460 (s), 1442 (s), 1303 (s), 1275 (s), 1131 (s), 1096 (m), 1022 (m), 935 (s), 901 (w), 864 (s), 759 (s), 719 (s), 696 (s), 669 (m), 560 (w). ¹H NMR (DMSO-d₆, 300 MHz) δ 4.99 (s, 4H), 5.20 (s, 4H), 8.00 (s, 4H); ¹³C NMR (DMSO-d₆, 75.48 MHz) δ 40.1, 40.3, 113.8, 128.6, 129.5, 160.9, 167.0. Elemental analysis calcd (%) for C₁₆H₁₂Cl₄N₂O₂ (406.08): C 47.56, H 2.98, N 6.90. Found: C 48.51, H 3.40, N 7.16.

Synthesis of 1,4-bis(4,5-bis(azidomethyl)isoxazol-3-yl)-benzene (14). To a solution of compound **13** (812 mg, 2.0 mmol, 1.0 equiv.), in water (50 mL) was added NaN₃ (1040 mg, 16.0 mmol, 8.0 equiv.) and the mixture was heated at 90 °C for 24 h. It was cooled to room temperature, and diluted with ethyl acetate (50 mL). The aqueous layer was extracted with ethyl acetate (3 × 50 mL) and washed with water (2 × 30 mL). The combined organic layer was dried over anhydrous Na₂SO₄ and concentrated *in vacuo*. The crude residue was triturated with chloroform-hexane (1 : 10) to give pure compound **14**. Brown solid. 726 mg, 84%, DSC (5 °C min⁻¹): 114 °C (mp), 207 °C (dec.). IR (KBr, cm⁻¹) 3064 (m), 2925 (m), 2112 (br s), 1721 (w), 1626 (m), 1439 (s), 1348 (s), 1281 (s), 1224 (m), 1167 (w), 1124 (w), 1005 (w), 968 (w), 915 (s), 878 (s), 863 (s), 790 (m), 767 (m), 687 (w), 654 (w), 547 (w). ¹H NMR (DMSO-d₆, 300 MHz) δ 4.65 (s, 4H), 4.94 (s, 4H), 7.93 (s, 4H). ¹³C NMR (DMSO-d₆, 75.48 MHz) δ 41.7, 42.9, 111.2, 128.7, 129.6, 161.3, 166.8. ¹⁵N NMR (50.70 MHz, DMSO-d₆): δ -5.7, -133.2, -165.6, -166.4, -305.7, -309.6. Elemental analysis calcd (%) for C₁₆H₁₂N₁₄O₂·0.5diethylether (469.43): C 46.06, H 3.65, N 41.77. Found: C 46.10, H 3.36, N 41.31.

Author contributions

S. L. conceptualization, investigation, methodology, and manuscript writing-original draft. R. J. S. X-ray data collection and structure solving. S. L. and J. M. S. conceptualization, manuscript writing-review and editing, supervision.

Conflicts of interest

There are no conflicts to declare.

Acknowledgements

The Rigaku Synergy S Diffractometer was purchased with support from the National Science Foundation MRI program (1919565). We are grateful for the support of the Fluorine-19 fund.

References

- H. Gao and J. M. Shreeve, *Chem. Rev.*, 2011, **111**, 7377–7436.
- (a) Q. Zhang and J. M. Shreeve, *Chem. Rev.*, 2014, **114**, 10527–10574; (b) H. Gao, Q. Zhang and J. M. Shreeve, *J. Mater. Chem. A*, 2020, **8**, 4193–4216; (c) S. Lal, R. J. Staples and J. M. Shreeve, *Chem. Eng. J.*, 2023, **452**, 139600.
- (a) T. M. Klapötke, *Chemistry of High-Energy Materials*, Walter de Gruyter GmbH & Co. KG, Berlin/New York, 2011, pp. 179–184; (b) S. Lal, L. Mallick, S. Rajkumar, O. P. Oommen, S. Reshmi, N. Kumbhakarna, A. Chowdhury and I. N. N. Namboothiri, *J. Mater. Chem. A*, 2015, **3**, 22118–22128.
- J. P. Agrawal and R. D. Hodgson, *Organic Chemistry of Explosives*, John Wiley & Sons, Ltd., Chichester, 2007, p. 243.
- (a) P. E. Eaton, R. L. Gilardi and M. X. Zhang, *Adv. Mater.*, 2000, **12**, 1143–1148; (b) P. E. Eaton, M.-X. Zhang, R. Gilardi, N. Gelber, S. Iyer and R. Surapaneni, *Propellants, Explos., Pyrotech.*, 2002, **27**, 1–6.
- J. V. Viswanath, K. J. Venugopal, N. V. S. Rao and A. Venkataraman, *Def. Technol.*, 2016, **12**, 401–418.
- (a) E. C. Koch, *Propellants, Explos., Pyrotech.*, 2015, **40**, 374–387; (b) A. F. Baxter, I. Martin, K. O. Christie and R. Haiges, *J. Am. Chem. Soc.*, 2018, **140**, 15089–15098.
- J. Akhavan, *The Chemistry of Explosives*, RSC Publishing, London, 3rd edn, 2011.
- (a) N. Fischer, D. Fischer, T. M. Klapötke, D. G. Piercey and J. Stierstorfer, *J. Mater. Chem.*, 2012, **22**, 20418–20422; (b) D. Trache, T. M. Klapötke, L. Maiz, M. A. Elghany and L. DeLuca, *Green Chem.*, 2017, **19**, 4711.
- T. M. Klapötke, *Energetic Materials Encyclopedia*, De Gruyter, Berlin/Boston, 2nd edn, 2021.
- P. W. Cooper, *Explosives Engineering*, Wiley-VCH, New York, 1996. ISBN 0-471-18636-8.
- K. G. Shipp, *J. Org. Chem.*, 1964, **29**, 2620–2623.
- (a) A. Sankaranarayanan, S. Lal, S. Rashmi, I. N. N. Namboothiri, A. Chowdhury and N. Kumbhakarna, *Fuel*, 2020, **282**, 118816; (b) A. Sankaranarayanan, S. Lal, I. N. N. Namboothiri, S. Rashmi, A. Chowdhury and N. Kumbhakarna, *Fuel*, 2019, **255**, 115836; (c) S. Lal, A. Bhattacharjee, A. Chowdhury, N. Kumbhakarna and I. N. N. Namboothiri, *Chem. – Asian J.*, 2022, **17**, e202200489; (d) S. Lal, A. Chowdhury, N. Kumbhakarna, S. Nandagopal, A. Kumar and I. N. N. Namboothiri, *Org. Chem. Front.*, 2021, **8**, 531–548.
- (a) P. Yin, Q. Zhang and J. M. Shreeve, *Acc. Chem. Res.*, 2016, **49**, 4–16; (b) P. Yin and J. M. Shreeve, *Adv. Heterocycl. Chem.*, 2017, **121**, 89–131.
- L. Bauer, M. Benz, T. M. Klapötke, T. Lenz and J. Stierstorfer, *J. Org. Chem.*, 2021, **86**, 6371–6380.
- P. J. Davies and A. S. Provatas, *Weapons systems. Characterisation of 2,4-dinitroanisole an ingredient for use in*



- low sensitivity melt cast formulations. *Science defence technology organization*, Edinburgh, Australia, 2006.
- 17 R. Banerjee, S. Maiti and D. Dhara, *Green Chem.*, 2014, **16**, 1365–1373.
 - 18 (a) L. A. Curtiss, K. Raghavachari, G. W. Trucks and J. A. Pople, *J. Chem. Phys.*, 1991, **94**, 7221–7232; (b) L. A. Curtiss, K. Raghavachari and J. A. Pople, *J. Chem. Phys.*, 1993, **98**, 1293–1298.
 - 19 M. J. Frisch, G. W. Trucks, H. B. Schlegel, G. E. Scuseria, M. A. Robb, J. R. Cheeseman, G. Scalmani, V. Barone, B. Mennucci, G. A. Petersson, H. Nakatsuji, M. L. Caricato, X. H. P. Hratchian, A. F. Izmaylov, J. Bloino, G. Zheng, J. L. Sonnenberg, M. Hada, M. Ehara, K. Toyota, R. Fukuda, J. Hasegawa, M. Ishida, T. Nakajima, Y. Honda, O. Kitao, H. Nakai, T. Vreven, J. A. Montgomery Jr., J. E. Peralta, F. Ogliaro, M. Bearpark, J. J. Heyd, E. Brothers, K. N. Kudin, V. N. Staroverov, R. Kobayashi, J. Normand, K. Raghavachari, A. Rendell, J. C. Burant, S. S. Iyengar, J. Tomasi, M. Cossi, N. Rega, N. J. Millam, M. Klene, J. E. Knox, J. B. Cross, V. Bakken, C. Adamo, J. Jaramillo, R. Gomperts, R. E. Stratmann, O. Yazyev, A. J. Austin, R. Cammi, C. Pomelli, J. W. Ochterski, R. L. Martin, K. Morokuma, V. G. Zakrzewski, G. A. Voth, P. Salvador, J. J. Dannenberg, S. Dapprich, A. D. Daniels, Ö. Farkas, J. B. Foresman, J. V. Ortiz, J. Cioslowski and D. J. Fox, *Revision D.01 ed*, Gaussian, Inc., Wallingford, CT, 2003.
 - 20 P. W. Atkins, *Physical Chemistry*, Oxford University Press, Oxford, 1982.
 - 21 M. S. Westwell, M. S. Searle, D. J. Wales and D. H. Williams, *J. Am. Chem. Soc.*, 1995, **117**, 5013–5015.
 - 22 H. Gao, C. Ye, C. M. Piekarski and J. M. Shreeve, *J. Phys. Chem. C*, 2007, **111**, 10718–10731.
 - 23 M. Suceśka, *EXPLO5 6.06*, Brodarski Institute, Zagreb Croatia, 2013.
 - 24 T. Lu and F. Chen, *Multiwfn*, *J. Comput. Chem.*, 2012, **33**, 580–592.
 - 25 (a) S. Lal, H. Gao and J. M. Shreeve, *New J. Chem.*, 2022, **46**, 16693–16701; (b) C. He, Y. Tang, L. A. Mitchell, D. A. Parrish and J. M. Shreeve, *J. Mater. Chem. A*, 2016, **4**, 8969–8973.
 - 26 (a) <https://www.bam.de>; (b) A ~25 mg sample was subjected to a drop-hammer test with a 5 or 10 kg dropping weight. The impact sensitivity was characterized according to the UN recommendations (insensitive, >40 J; less sensitive, 35 J; sensitive, 4 J; very sensitive, 3 J) (c) UN, Committee of Experts on the Transport of Dangerous Goods, *Recommendations on the transport of dangerous goods, manual of tests and criteria*, United Nations, New York, 5th revised edn, 2009.
 - 27 P. R. Spackman, M. J. Turner, J. J. McKinnon, S. K. Wolff, D. J. Grimwood, D. Jayatilaka and M. A. Spackman, *J. Appl. Crystallogr.*, 2021, **54**, 1006–1011.
 - 28 G. M. Sheldrick, *Acta Crystallogr., Sect. C: Struct. Chem.*, 2015, **71**, 3–8.
 - 29 O. V. Dolomanov, L. J. Bourhis, R. J. Gildea, J. A. K. Howard and H. Puschmann, *J. Appl. Crystallogr.*, 2009, **42**, 339–341.

